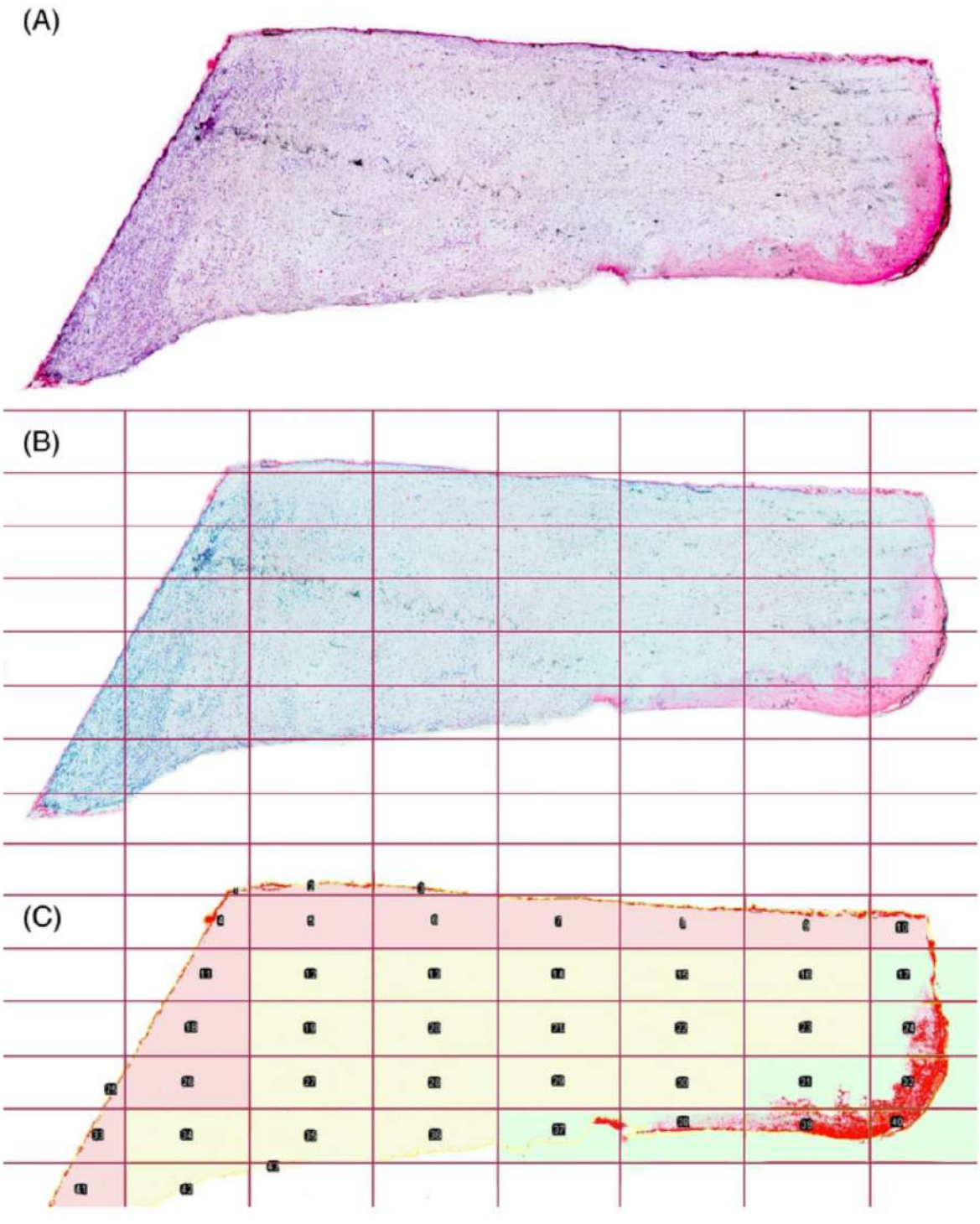
(A)
(B)
(C)

Received: 11 June 2023 | Revised: 27 September 2023 | Accepted: 30 September 2023

DOI: 10.1111/cid.13286

WILEY

ORIGINAL ARTICLE

Effect of argon plasma abutment activation on soft tissue healing: RCT with histological assessment

Luigi Canullo[1,2] | Antonacci Donato[3] | Paolo Savadori[4,5] | Sandro Radovanovic[6] | Roberta Iacono[7] | Mia Rakic[8]

[1]Department of Surgical Sciences (DISC), University of Genoa, Genova, Italy

[2]Department of Periodontology, University of Bern, Bern, Switzerland

[3]Private Practice, Bari, Italy

[4]Department of Biomedical, Surgical and Dental Sciences, Università Degli Studi di Milano, Milan, Italy

[5]Fondazione IRCCS Ca' Granda Ospedale Maggiore Policlinico, Maxillo-Facial Surgery and Dental Unit, Milan, Italy

[6]Faculty of Organizational Sciences, University of Belgrade, Belgrade, Serbia

[7]Department of Oral and Maxillo-facial Sciences, Sapienza University of Rome, Rome, Italy

[8]Facultad de Odontologia, Etiology and Therapy of Periodontal Diseases (ETEP) Research Group, Universidad Complutense de Madrid, Madrid, Spain

Correspondence
Luigi Canullo, Department of Surgical Sciences (DISC), University of Genoa, Largo R. Benzi 10, 16132 Genoa, Italy.
Email: luigicanullo@yahoo.com

Abstract

Objective: To assess the peri-implant soft tissue profiles between argon plasma treatment (PT) and non-treated (NPT) healing abutments by comparing clinical and histological parameters 2 months following abutment placement.

Materials and Methods: Thirty participants were randomly assigned to argon-plasma treatment abutments group (PT) or non-treated abutments (NPT) group. Two months after healing abutment placement, soft peri-implant tissues and abutment were harvested, and histological and clinical parameters including plaque index, bleeding on probing, and keratinized mucosa diameter (KM) were assessed. Specialized stainings (hematoxylin–eosin and picrocirious red) coupled with immunohistochemistry (vimentin, collagen, and CK10) were performed to assess soft tissue inflammation and healing, and the collagen content keratinization. In addition to standard statistical methods, machine learning algorithms were applied for advanced soft tissue profiling between the test and control groups.

Results: PT group showed lower plaque accumulation and inflammation grade (6.71% vs. 13.25%, respectively; p-value 0.02), and more advanced connective tissue healing and integration compared to NPT (31.77% vs. 23.3%, respectively; $p = 0.009$). In the control group, more expressed keratinization was found compared to the PT group, showing significantly higher CK10 (>47.5%). No differences in KM were found between the groups.

Significance: PT seems to be a promising protocol for guided peri-implant soft tissue morphogenesis reducing plaque accumulation and inflammation, and stimulating collagen and soft tissue but without effects on epithelial tissues and keratinization.

KEYWORDS

abutments, argon plasma, collagen, cytokeratin 10, decontamination, MLA, peri-implant soft tissues, vimentin

Summary Box

What is known

Several in vitro and preclinical studies have shown beneficial effects of argon plasma (PT) treatment on soft tissue.

What this study adds

This study adds evidence on the effects of PT on peri-implant soft tissue healing and suggests that PT provides more advanced connective tissue healing than untreated abutments. The peri-implant soft tissues around the PT abutments reduce plaque accumulation and inflammation. PT does not affect peri-implant epithelial tissues and keratinization.

1 | INTRODUCTION

Soft peri-implant tissues play the first line of defense against microbiological threats responsible for the advent of peri-implant disease, so the robustness of the peri-implant soft tissue seal is recognized as a key factor in the long-term maintenance of peri-implant health.[1] As this, soft tissues are in the spotlight of the current implant research, particularly the aspect concerning the initial soft tissue healing as the first stage of soft tissue integration. The key elements of the peri-implant soft tissue phenotype (PiSP) are mucosal thickness, keratinized mucosa width (KMW), and/or supracrestal tissue height.[2] It is considered that thick biotype and wider KMW better preserve soft and hard peri-implant tissues, by preventing recession, biofilm accumulation, and related apical propagation, while stabilizing peri-implant bone remodeling.[3,4] As the PiSP is site-specific and susceptible to changes over time, local factors in particular[2] plaque accumulation, prosthetic factors, contaminants, and abutments surface characteristics are thoroughly investigated lately with the main objective of developing new strategies for optimal soft tissue integration.[5,6] The soft tissue healing process as an inherent stage of soft tissue integration relies on inflammatory reactions while macrophage polarization currently attracts great attention as being recognized as a critical determinant of the soft tissue integration fate.[7] In brief, the pro-inflammatory M1 macrophages are involved in initial healing processes mostly for removal of the tissue debris and cloth that occurred within the surgical intervention, which should be optimally replaced by the M2 pro-regenerative macrophages responsible for tissue formation and optimal soft tissue integration.[8,9] Macrophage polarization and repolarization are highly dependent on local factors that might interfere with M2 polarization, leading to imperfect soft tissue integration on the titanium surface[7] with decreased resistance and increased susceptibility to biological complications.[10] Thus, modification of the clinical protocols and implant surface treatments providing optimal healing conditions and suppression of negative factors such as sub-clinical infection are ongoing priorities in oral implantology and regenerative medicine in general.[11,12]

The standard prosthetic workflow implying multiple soft tissue disconnections at critical time points of the biological phases of soft tissue integrations within abutments exchanges, impressions, fitting, and final prosthetic delivery is considered to lead to the imperfect soft tissue integration associated with long junctional epithelium.[13]

Additionally, the lack of periodontal ligament within the peri-implant soft tissues initially makes the soft tissues less resilient in the absence of periodontal fibers. Recent studies highlight the impact of the lack of connective tissues on the overall local biology, particularly on the decreased defensive and regenerative potential, and increased susceptibility to immunopathologies.[14]

Plasma treatment (PT) of dental implant surfaces received increasing attention lately due to its outstanding capacity of removing surface contaminants more successfully than other available protocols.[15] PT provides wide antimicrobial effects, with proven effectiveness against highly virulent bacteria associated with peri-implantitis.[16–18] Finally, PT activation enhances implant surface wettability thus stimulating cell migration and adhesion to the implant surface,[19–21] and promoting cell attachment with proportionally accelerated hard and soft tissue integration.[17,22–24] Regarding soft tissues specifically, in vitro studies have demonstrated the capacity of the argon plasma to increase migration, proliferation, and adhesion of human fibroblasts, and pro-stimulative effects on soft tissue integration and angiogenesis.[25–27] Additionally, the anti-biofilm effects of the PT abutment pre-treatment at the clinical and microbiome levels were previously demonstrated in the proof-of-concept study reported by this group.[28] Nevertheless, although a great number of in vitro and pre-clinical studies reported on the beneficial effects of argon plasma treatment of soft tissues, respective clinical confirmation is still lacking.

Thus, the working hypothesis was that argon plasma abutment pre-treatment would provide pro-stimulative effects on peri-implant soft tissue healing compared to no treatment.

The objective of the present study was to compare the peri-implant soft tissue profiles between argon plasma pre-treated and non-treated healing abutments by comparing clinical and histological parameters of the peri-implant soft tissues 2 months after abutment placement.

2 | MATERIALS AND METHODS

2.1 | Study design and regulatory aspects

The present study was designed as a randomized clinical study aiming to evaluate the effects of argon plasma abutment treatment on peri-implant soft tissue healing and integration. The influence of the surface treatment was assessed comparing clinical and histological parameters between the two groups. Another goal of this study was to collect data on complex soft tissue profiles around treated and non-treated healing abutments, in addition to standard statistics, the predictive models based on clinical and histological parameters were generated using machine learning algorithms (MLAs). To convincingly simulate a standard clinical setting, an equal number of abutments with smooth surfaces were distributed between the test and control groups.

Patients were recruited and treated in a private dental practice (Rome, Italy) between June and December 2021. The research protocol was approved by the local ethics committee (Comitato Etico Lazio 1, ref. number 813, accepted on June 18, 2021). The participants were informed of the procedures and accepted to contribute by signing an informed consent form. The study was conducted in accordance with the Good Clinical Practice (GCPs) guidelines and the Declaration of Helsinki of 1975, as revised in 2013.[29]

The study was registered on the site clinicaltrial.com under the reference NCT05821673.

2.2 | Study population, criteria, and randomization

Following the initial eligibility assessment of 40 patients undergoing implant therapy with immediate healing abutment connection, the final study sample included 30 participants.

The inclusion criteria were: the presence of at least 4 mm of keratinized mucosa around the implants, patients aged 18 years or older, medically healthy patients (ASA I), or patients with mild systemic disease (ASA II); partially edentulous state; healthy periodontal condition (also including periodontal health on reduced periodontium) according to the referent case definition. Exclusion criteria included: ASA physical status ≥3, severe smokers (>10 cig/day), patients undergoing bisphosphonate therapy, pregnant or lactating women, estrogen-related hormonal disorders or hormonal substitution therapy, untreated periodontitis (pocket depth ≥4 mm with positive bleeding on probing [BoP]), multiple gingival recession, and patients with a history of head and neck cancers and radiotherapy in this region.

Participants underwent two-level randomization for allocation of healing abutments with different surface configurations and experimental treatment using permuted block technique to limit any selection bias. Allocation concealment was preserved by sealing the tested abutments in sterile envelopes sealed in opaque sleeves opened at the time of the second surgical step.

2.3 | Surgical procedures

After local anesthesia, the baseline thickness of the keratinized mucosa was clinically assessed with a periodontal probe. A conventional surgical procedure with a mid-crestal incision and gentle lifting of a full-thickness flap was performed. The Premium One implant (Sweden & Martina) was used. This implant presents a neck with the ultrathin threaded microsurface treatment, a special micro-roughening, and an implant body surface treated with a zirconium oxide blasting treatment coupled to a mineral acid etching treatment. The diameter of the inserted implants was 5 mm, with an internal connection diameter of 3.3 mm. All implants were placed at the bone level and their diameter was 5 mm, connected to the prosthetic component through an internal hex connection with a diameter of 3.3 mm (Figure 1).

Depending on the assigned study group, a specifically designed healing abutment was screwed in at 20 N. The flaps were sutured around the abutment in order to create an intimate surface contact between them. Participants received healing abutments with machine surface, characterized by circular micro-threads with a furrow of less than 2 μm (surface roughness: Ra = 0.2 and Sa = 0.11).

Immediately before surgeries, healing abutments allocated to the test group were placed in an Argon plasma reactor (Diener Electronic GmbH, Jettingen, Germany) for decontamination and activation. In

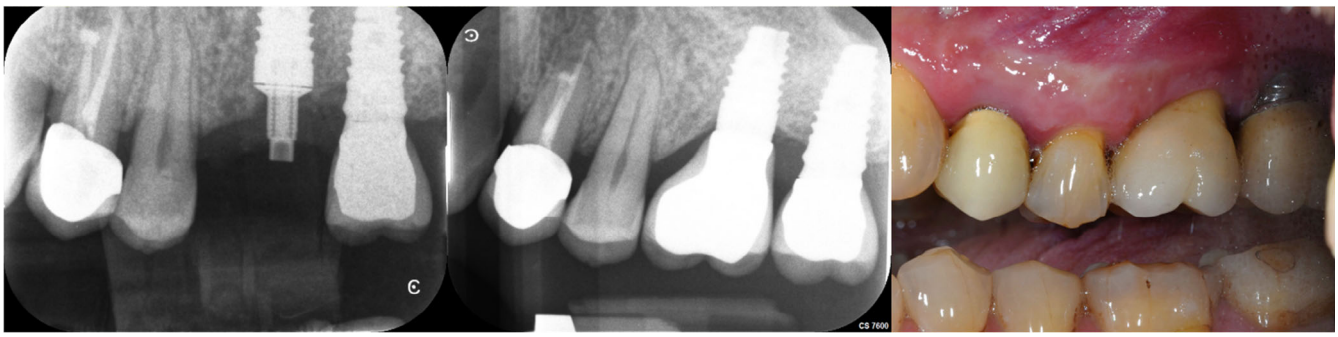

FIGURE 1 Implant-prosthetic rehabilitation.

order to restrict any post-treatment contamination, abutments were inserted immediately after the end of the plasma process. The reactor was set at 75 W of power and −10 MPa of pressure for 12 min.

2.4 | Clinical measurements

Two months after healing abutment placement, the plaque index (PI) and BoP[30,31] were assessed 48–72 h before the biopsy. Their scores were recorded at six points around each abutment. The result obtained were averaged and expressed in percentage. Clinical measurements were performed using a plastic probe graded in millimeters (Williams Colorvue Probe, Hu-Friedy, Chicago, IL) applying the light force (15 N/cm force). All measurements were performed by one experienced examiner (LC) after a calibration exercise demonstrating 98.6% concordance based on 10 serial measurements of BoP.

2.5 | Soft tissue biopsies

Soft tissue biopsies were harvested by a circumferential guided biopsy that contained soft peri-implant tissues around the abutment and the abutment itself. The harvesting technique and abutment design were explained in the previous article.[32] In brief, a guide pin was attached to the abutment allowing a 5-mm diameter circular blade to cut apically to the interface with the implant. Thus, a 1.3 mm circumferential thickness of keratinized mucosa was excised together with the abutment, while the new smooth, 5-mm-wide healing abutment was screwed in place of the retrieved one. The biopsies were preserved in neutral formalin and transferred immediately to the laboratory for analysis.

2.6 | Histological assessment

Soft tissue biopsies were fixed in 10% buffered formalin, and dehydrated in a graded series of ethanol, rinsed, and embedded in a glycol-methacrylate resin (methyl-methacrylate).

After polymerization, samples were sectioned along the mid-longitudinal axis of the trephine cylinder by means of a high-precision diamond saw (Struers Secotom 50, Cleveland, OH, USA). Histologic sections of the tissue were performed using a laser microtome (TissueSurgeon, LLSROWIAK LaserLabSolutions GmbH, Hannower, Germany) in sections of 5 µm and stained by means of specialized stainings and immunohistochemistry (IHC). Standard hematoxylin and eosin (H&E) staining was used for standard histopathological assessment and inflammatory grading. Picrosirius red staining and collagen immunostaining were performed for assessment of the collagen profile. CK10 was used to estimate the degree of keratinization while vimentin was used to assess the soft tissue healing.[33–36] Vimentin was measured using a commercial antibody (identify vimentin ab8978 primary antibody, Abcam, Cambridge, UK). Antigen demasking using Tris Etilen diamino tetra acetic acid at pH 9 for 4 h at 60°C. CK10 was detected using a commercial antibody (ab9026-Abcam, Cambridge, UK) with antigen demasking using citrate buffer at pH 6 for 4 h at 60°C. The secondary antibody was the same for both primary antibodies (Alkaline phosphatase Mouse & Rabbit Kit [Fast Red]), ready to use MEDAC (Wedel, Germany).

The stained slides were scanned and converted into digital formats using a slide scanner (Nanozoomer Digital Pathology, NDP slide scanner, Hamamatsu Photonics, Japan). The tissue's microanatomy was analyzed through H&E staining. Particularly, attention was focused on cellular stress features like nucleus dimension, cellular thickness, and shape. The H&E staining was also used to obtain a semi-quantitative assessment of inflammation levels present in the tissue. To obtain this value, the area occupied by inflammatory infiltrates was defined as the region of interest (ROI). Analysis for quantification of inflammatory levels and subsequent quantitative analyses were conducted using the Fiji-ImageJ program (NIH, Bethesda, Maryland; https://imagej.nih.gov/ij/), equipped with the IHC profiler plugin.[37,38] The regions containing inflammatory cells were outlined to obtain the value of the area occupied in terms of pixels, and this value was then normalized to the total area of the examined sample, also expressed in pixels (Figure 2C). This procedure allowed obtaining a percentage value that could be compared across different samples, as it is relative rather than absolute and independent of the size of the sample itself.[39] Collagen stained by picrosirius red staining, was quantified through color deconvolution. Collagen quantification was expressed as a proportion of collagen-occupied surface and the total sample surface. The reddish part of the sample, corresponding to collagen, was taken as the ROI, and through color deconvolution, only this color channel was selected. Thereafter, quantification was performed by setting a colorimetric threshold value to exclude tissues that were not collagenous.[40] Vimentin and CK10 were measured with color deconvolution using a plug-in software for Fiji-ImageJ called color deconvolution 2, developed by Birmingham University (https://blog.bham.ac.uk/intellimic/g-landini-software/colour-deconvolution-2/) based on the algorithm made by Ruifork.[41] This software isolates the chromogenic substrate signal generated from the secondary antibody and permits its quantification by setting a threshold value. In the case of CK10, the three-level spatial distribution was additionally performed, given the specificity of keratinization. Each sample image was divided into regular-sized quadrants by a grid. The horizontal and vertical lines of the grid were spaced from each other by a length equal to 12.5% of the total length of the image to define the three areas: abutment-oriented, central, and epithelial zones, in order to perform CK10 quantification for each zone (Figure 2).

Two blinded examiners (LC, DA) previously calibrated on 10 samples, their linear inter-examiner weighting coefficient is $k = 0.965$, performed IHC analysis and recession assessment. The captured images had no reference to the assigned group and were identified by a code.

2.7 | Data management

Sample size calculation was performed for the PI values estimated in the previous study with a similar design.[28] According to that, a total

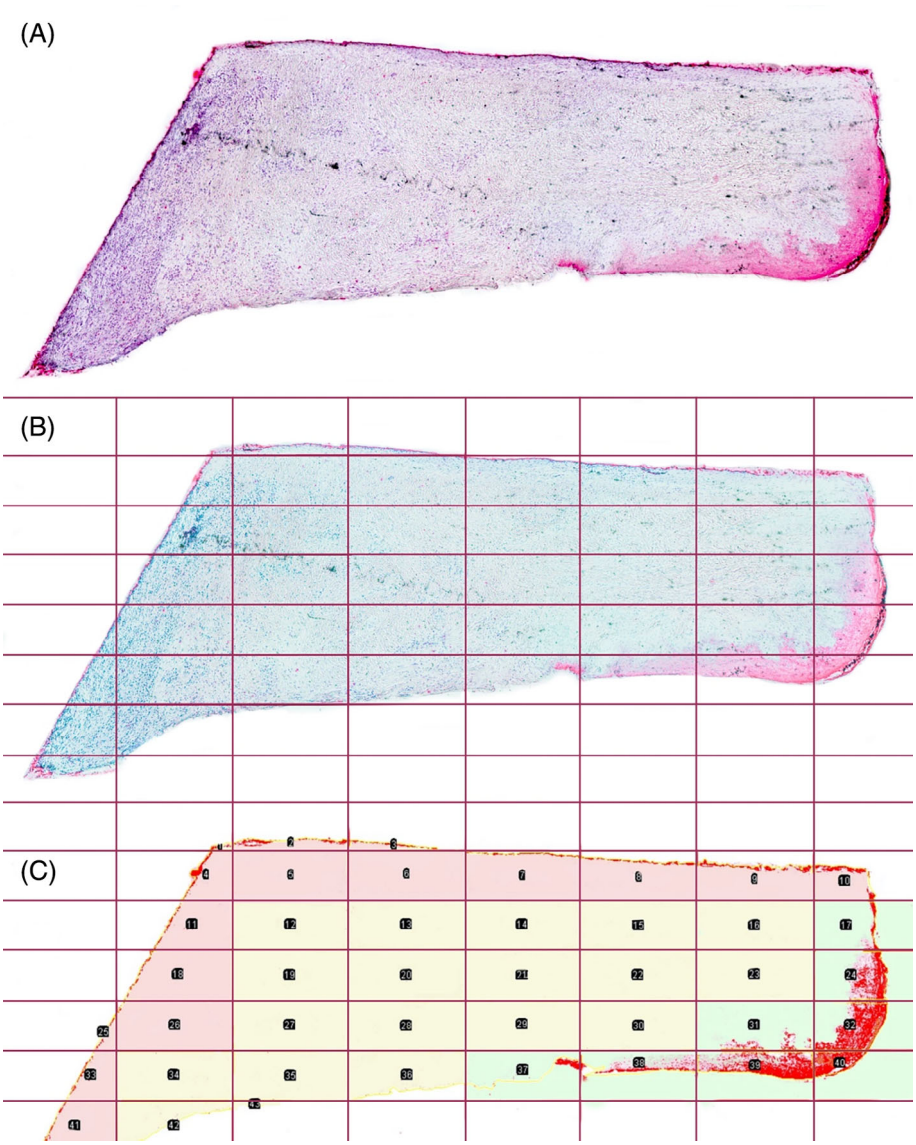

FIGURE 2 Illustrates of the various steps of immunohistochemistry (IHC) quantification of target cytokeratins. In image (A), IHC staining reveals the presence of CK10 around the free gingival margin and at the abutment interface. In image (B), the slide was divided into rectangular regions of interest (ROI) of the same size, and the staining intensity in each rectangle was measured, in this way, the quantification was independent of the size of the gingival specimen. The image (C) shows the ROIs that were numbered and divided into three areas: the area near the abutment, the middle area, and the area of the free gingival margin.

sample of 30 participants using α of 0.05 would result in a power of 0.8 with a drop-out of 25%. Demographic characteristics between the groups were analyzed using Fisher's exact test.

Clinical parameters and the proportion of IHC-positive cells and collagen per sample were expressed as median ± standard deviation and were further compared using the Mann-Whitney *U* test between the groups. Statistical analysis was performed using commercial software (SPSS v.25.0; SPSS Inc., USA). To assess whether PT and NPT exert distinctive overall profiles based on composite clinical and histological parameters, decision trees were generated as a type of easily interpretable MLA. The five-fold cross-validation was performed. The dataset was divided into five random subsets (i.e., five different sets of random patients), and decision trees were further trained on four subsets, while the predictive performance of the model was estimated on the remaining one. The procedure was repeated five times so that each subset was used exactly once for the evaluation of the model. As a result, five results were obtained for each performance and the metric average value with standard deviation was reported.[42] The predictive model was evaluated based on accuracy, area under the Receiver operating Characteristc (ROC) curve (AUC), precision, and recall metrics. The predictive model was developed using C4.5 decision trees.[43]

3 | RESULTS

Demographic characteristics, including age and gender, were similarly distributed between the groups ($p > 0.05$) (Table 1).

3.1 | Clinical outcomes

The effect of PT on clinical parameters and soft tissue phenotype is provided in Table 2. PT was associated with lower plaque accumulation, while respective effects on BoP and soft issue phenotype were similar to the NPT.

TABLE 1 Demographic characteristics.

	NPT ($n = 15$)	PT ($n = 15$)
Age mean	55.38	50.04
Male	8	9
Female	7	6
Mandible	5	7
Maxilla	10	8

Abbreviations: NPT, non-plasma treated; PT, plasma treated.

3.2 | Histological outcomes

The assessment of inflammatory infiltrate in the H&E stained samples showed higher inflammation in the NPT compared to PT according to a higher proportion of inflammatory cells (13.25% vs. 6.71%, respectively; *p*-value 0.02) (Figure 3). NPT showed less collagen compared to the test group: 23.3% versus 31.77%, respectively ($p = 0.009$). Moreover, the total collagen amount (%) was greater in the PT group when compared to NPT ($p = 0.038$) as well as vimentin ($p = 0.003$) indicating more intense

TABLE 2 Clinical and histological parameters between the groups.

Parameters	NPT (15)	PT (15)	*p*-Value (95% CI)
Clinical parameters			
BoP	0	0	0.461 (−0.001, 0.999)
PI	2.45 ± 1.54	1.45. ± 1.58	**0.035*** (**0.106, 2.999**)
Phenotype			
Thickness (mm)	2.75 ± 1.1	2.5 ± 0.8	0.882 (−0.500, 0.500)
KT diameters (mm) before	3.3 ± 1.2	3.8 ± 1.4	0.239 (−1.000, 0.165)
KT diameters (mm) after	3.4 ± 1.7	3.9 ± 1.2	0.141 (−1.000, 0.179)
Histological parameters			
Inflammatory infiltrate (%)	2.31 ± 0.70.	2.00 ± 0.93.26	0.430 (−0.13, 1.00)
Collagen content (%)	25.92 ± 10.31	33.37 ± 9.33	**0.038*** (**−17.38, −0.16**)
Immunohistochemical markers			
Vimentin %	35.3 ± 15.7	59.5 ± 5.1	**0.003*** (**−46.6, −10.4**)
Collagen %	23.9 ± 3.4	31.7 ± 2.7	**0.038*** (**−17.380, −0.160**)
CK10%	6.51 ± 1.7	2.69 ± 1.2	**0.005*** (**0.999, 5.835**)
CK10 abutment %	21.5 ± 10.2	38.1 ± 8.4	0.064 (−0.750, 96.519)
CK10 center %	72.2 ± 8.7	10.4 ± 6.2	**0.004*** (**16.942, 93.077**)
CK10 epithelium %	73.0 ± 9.3	69.2 ± 8.6	0.245 (−29.596, 96.038)

Note: Values are expressed as median ± standard deviation. Bold indicates statistical significance.
Abbreviations: BoP, bleeding on probing; CI, confidence interval; KT: keratinized TIssue; NPT, non-plasma treated; PI, plaque index; PT, plasma treated.
*$p < 0.05$: NPT < PT: vimentin, collagen; NPT > PT: total CK10 and CK10 center.

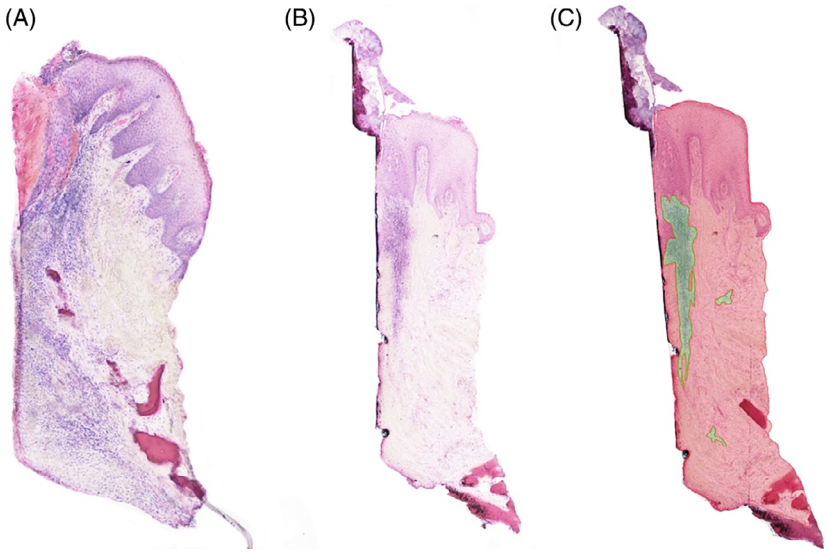

FIGURE 3 Inflammation. Samples stained with hematoxylin and eosin. (A) Untreated sample, (B) treated sample. In the untreated sample, it is possible to see a greater quantity of inflammatory infiltrates as well as hypertrophy in the multilayered keratinized tissue. (C) Representation of the semiquantitative measurement of inflammation level.

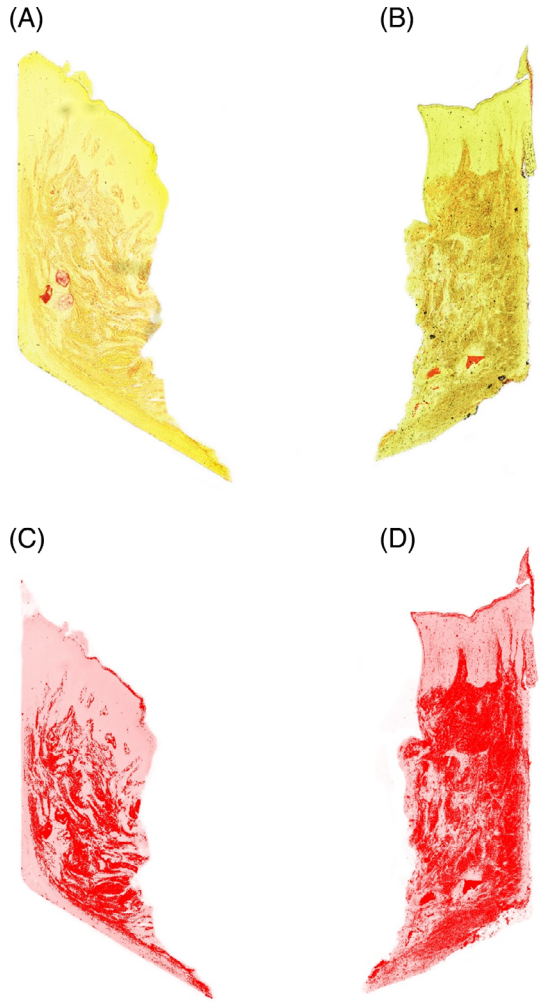

FIGURE 4 Picrosirius red. Images relating to collagen staining using Sirius red. (A) Untreated sample, (B) treated sample; (C) and (B) images processed with ImageJ using color deconvolution to isolate the red-colored collagen from the yellow-colored background for collagen quantification.

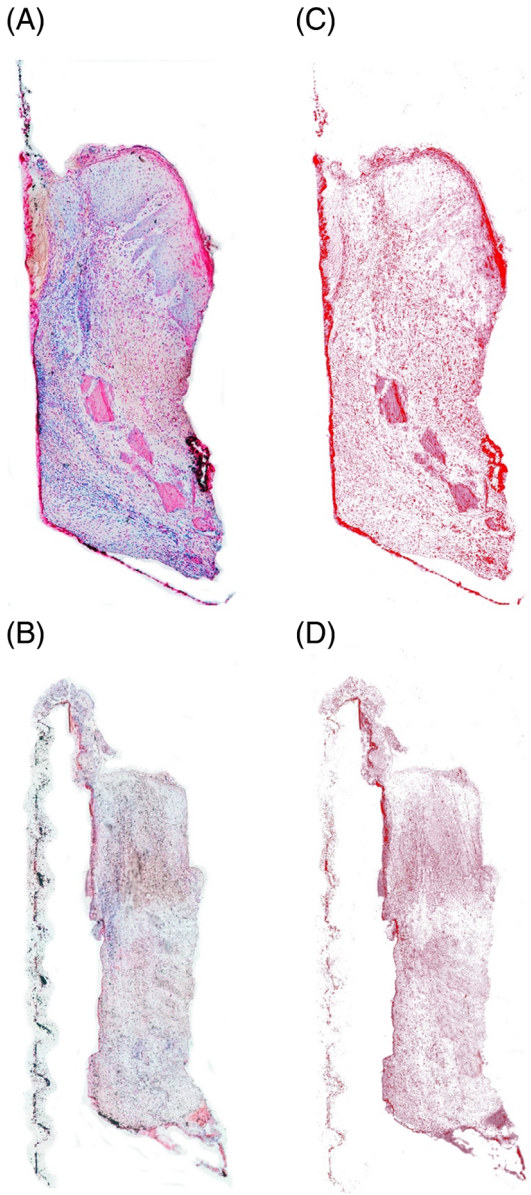

FIGURE 5 CK10. Images relating to the CK10 antibody. (A) Immunohistochemistry relating to an untreated sample, (B) immunohistochemistry relating to a treated sample; (C), (D) images processed with ImageJ with color deconvolution to isolate the chromogenic signal given by the fast red.

connective tissue formation in PT (Figure 4). A high concentration of vimentin indicates an actively healing tissue. CK10 was significantly more expressed in NPT when compared to PT ($p = 0.005$) suggesting less pronounced keratinization in the experimental group. Given the specificity of keratinization, the grade of CK10 was assessed in three regions and the central zone showed the most expressed keratinization in NPT ($p = 0.004$) while the abutment-oriented and epithelium showed a comparable degree of keratinization between the groups (Figure 5).

3.3 | Peri-implant soft tissue profiles around PT and NPT healing abutments

The predictive model generated based on clinical and immunohistochemical parameters discriminated PT and NPT with high accuracy (accuracy: 0.868 ± 0.091; precision: 0.920 ± 0.160, recall: 0.850 ± 0.123 and AUC = 0.938 ± 0.069) and it is depicted in Figure 6. NPT was associated with a high percentage of CK10 (>47.5%), or in the case of less CK10, with thin biotype and higher vimentin expression (>40.45%) or thick biotype and higher keratinized mucosa (KM) diameter. PT was associated with lower CK10 expression (<5.97%) and high vimentin expression (>47.5%), or in case of lower vimentin expression (<40.45) PT was associated with thin biotype and lower vimentin, or with thick biotype and lower KM diameter (<2.5 mm).

4 | DISCUSSION

The present study has demonstrated that pre-treatment of the abutment with argon plasma helped to reduce plaque accumulation and

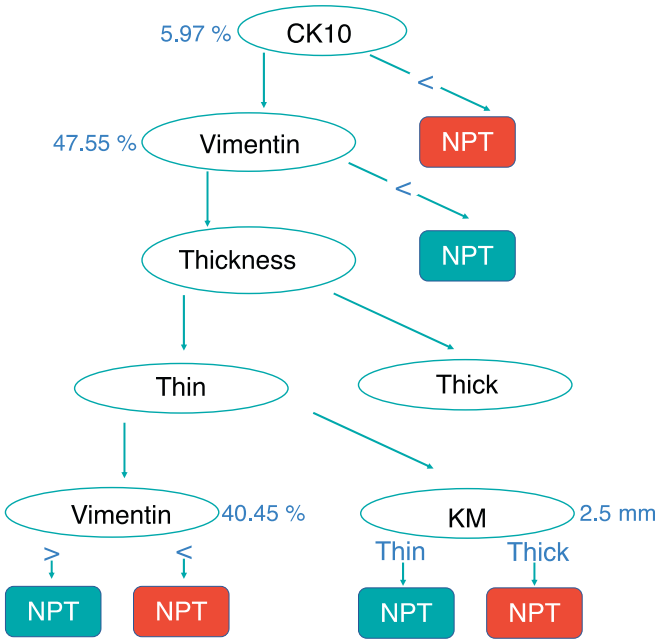

FIGURE 6 Soft tissue profiles around plasma-treated and non-treated abutments. NPT was associated with a high percentage of CK10 (>47.5%), or in the case of less CK10, with a thin biotype and higher vimentin expression (>40.45%) or thick biotype and higher keratinized mucosa diameter. PT was associated with lower CK10 expression (<5.97%) and high vimentin expression (>47.5%), or in case of lower vimentin expression (<40.45) PT was associated with thin biotype and lower vimentin, or with thick biotype and lower keratinized mucosa diameter (<2.5 mm). Model provided accuracy: 0.868 ± 0.091; precision: 0.920 ± 0.160, recall: 0.850 ± 0.123 and area under the ROC curve = 0.938 ± 0.069. PT, plasma treated; NPT, non-plasma treated; KM, keratinized mucosa; thresholds are provided in blue.

the degree of inflammation, while providing pro-stimulative effects on peri-implant connective tissue healing and integration, based on significantly higher collagen formation and vimentin expression than the control group. In turn, the control group showed more expressed keratinization than the PT, based on significantly higher CK10 expression, although the diameter of the keratinized mucosa was similar between the groups at the clinical level.

In vitro and in vivo studies have clearly indicated that the physico-chemical characteristics of the abutment surface influence and shape peri-implant soft tissue integration, but it has also been suggested that materials influence host and bacterial cell attraction.[44,45] Hence, the development of a fine-tuned protocol that promotes soft tissue integration while preventing bacterial adhesion to the implant surface is a priority but also a challenging request, and the outcomes of the present study suggest the promising capacity of PT to respond to it.

It has been proposed that the success of the implant treatment can be predicted based on "competition" between bacterial and soft tissue cells, as bacterial biofilms interfere with macrophage polarization and prevent epithelial cells from sealing to the implant surface. The present study showed that PT helped to reduce plaque accumulation and inflammation, in accordance with the study previously reported by this group.[28] Briefly, the previous study showed the same clinical results between the groups, while demonstrating that bacterial biofilms around PT were dominated by pioneer colonizers in contrast to NPT which was associated rather with late colonizers characteristic to mature biofilms.[28]

This is important because infection, even in its sub-clinical grade, is considered the most devastating complication of biomaterials[46] due to its immediate interference with healing processes and far-reaching role in the development of future implant infections.

Another plausible explanation for the lower inflammation in PT compared to NPT can be explained by the capacity of this treatment to remove surface contaminants and pollutants also originating from the standard manufacturing process, such as metal particles, grease, hydrocarbon, etc.[47,48]

As it was demonstrated that healing abutments affect immunological networks within healing processes, it might be considered that the reduction of pollutants would support the healing process by promoting M2 polarization and guiding the inflammatory reactions toward a regenerative course.

Briefly, the single clinical parameter that was significantly lower in the PT group when compared to NPT was PI, suggesting the anti-biofilm effects of the PT. This result is in accordance with the study previously reported by this research group, demonstrating that plasma pre-treatment of abutments decelerates plaque accumulation and maturation[28] at both the clinical and microbiome levels.

In that sense, control of the biofilm via plasma-activated surface may provide favorable effects on M2-macrophage polarization underlying soft tissue healing processes.[49] Additionally, one of the key PT minute of angle is the increase of surface wettability, and it has been reported that hydrophilicity of the implant surface improves soft tissue integration through the promotion of the M2-polarization and upregulation of the gingival fibroblasts.[11]

CK10 is a standard biomarker of keratinization used to estimate the grade of keratinization of the peri-implant epithelium.[50] The present study has demonstrated significantly more expressed CK10 in NPT when compared to PT, but the level of KM diameter was clinically comparable between the groups. The analysis of microanatomy showed no tissue alteration in either group, except for a slight hypertrophy of the nuclei in the NPT, characterized by a compact gingival epithelium without cell spacing and a solid subgingival connective tissue structure.

In that context, the significantly more expressed CK10 in NPT can plausibly be considered as the predominance of the reparatory phase in peri-implant soft tissue healing around NPT, as cytokeratin family includes fibrillar proteins involved in scar tissue formation.[51] This observation is also supported by the findings obtained with picrosirius red staining, which shows that tissues with a higher level of CK10 have a minor quantity of collagen and vice versa.

Finally, collagen improves elasticity and tensile strength to tissues and is indicative of a functional healing process with a predominant regenerative component,[52] and collagen content was significantly more expressed in PT specimens. Moreover, vimentin, a type III

intermediate filament protein constituting the cytoskeleton and bringing strength and mechanical resistance to the cell, was expressed in mesenchymal cells and plays a pivotal role in the healing processes.[28–31] In fact, vimentin is a structural protein of the cytoskeleton that provides strength and mechanical resistance to the cell. It plays a pivotal role in wound healing, as it was demonstrated that transgenic mice lacking vimentin have longer healing times when compared to wild-type animals.[28] Vimentin is highly expressed in mesenchymal cells and cells going through the epithelial–mesenchymal transition during wound healing, fibrosis, and metastatic tumoral processes.[29–31] For these reasons, vimentin is considered one of the gold standard markers of the healing processes. This pro-healing marker was significantly more expressed in PT compared to NP, additionally suggesting more potent healing processes and more robust soft tissue integration around PT pre-treated abutments. This is indirectly in accordance with reported in vitro studies showing the capacity of PT to increase migration, proliferation, and adhesion of human fibroblasts to the implant surface, improving the overall quality of the soft tissue integration.[22–24] This is also concordant with findings reported by Garcia and colleagues,[53] demonstrating stronger connective tissue attachment following plasma treatment, with more densely packed collagen fibers and a fair prevalence of oblique fibers. These findings can also be assigned to the biophysical properties of the argon plasma and its ability to increase the surface energy abutment wettability.[54–56]

In fact, while this process prevents microscopical changes in titanium topography, it simultaneously allows the treated surfaces to act as a "cell multiplier."[57–61] The recently published histological study indeed demonstrated increased absorption of proteins and cellular adhesion with cells spreading around bioactivated abutments, and a significantly wider band of connective tissue in contact with pre-treated abutments even in the early-stage healing.[32] This is of particular importance since the main objective of peri-implant soft-tissue management is to increase the fibroblast and extracellular matrix content to the peri-implant connective tissues exhibiting less gingival fibroblasts compared to the gingival tissue around natural teeth. In that context, the experimental PT seems to answer the requests for peri-implant soft tissue "reinforcement" using a low invasive procedure in contrast to the standard surgical procedure of connective tissue grafting also associated with post-operative morbidity.

To perform comprehensive and highly accurate peri-implant soft tissue profiling between PT and NPT, the present study deployed MLAs in addition to conventional statistical methods. As recently stated, there are many ways in which MLAs support medicine thanks to their outstanding capacity in the assessment of large datasets, with superior accuracy compared to standard statistics and their ability to identify complex interrelations and to implement them into interpretable patterns and clinical strategies.[62] The generated MLA model exerted solid properties and the critical discriminants between PT and NPT were higher CK10 expression in NPT and higher vimentin in PT groups. This result is in agreement with the statistical results, and considering all the outcomes as a whole, these outcomes are suggestive of more expressed soft tissue reparative healing around NPT and more functional regenerative healing around PT abutments. However, further studies are needed to confirm this hypothesis.

The present study has several limitations. The main ones are the relatively small sample size and lack of longitudinal follow-up, which should be the subject of future studies. Although the experimental and test groups had a comparable distribution of implant positions per jaws, studies with larger samples should also reveal the potential impact of different implant positions within jaws on PT efficacy. Another limitation of the study is the evaluation of only one type of abutment surface, so future studies should evaluate the effect of PT on different types of abutments, particularly on rough abutment surfaces with a special focus on their respective anti-plaque properties. Finally, the present study investigated only titanium abutments, while in light of recently published systematic reviews and their related favorable findings on ceramic abutments,[63,64] the forthcoming research on the PT protocols should extend to other materials as well.

5 | CONCLUSION

Within the limitations of the study, the healing abutment PT provides less plaque accumulation and inflammation, with more robust connective tissue healing but without effects on keratinized epithelium when compared to the control group. Hence, PT seems to be a promising tool for guided soft tissue morphogenesis and potent soft tissue integration.

AUTHOR CONTRIBUTIONS

Luigi Canullo: conception, design, data collection, drafting and critical revision of the article; Donato Antonacci data curation, investigation, and methodology; Paolo Savadori investigation, data curation, and methodology; Radovanovic Sandro statistics; Roberta Iacono writing—review and editing; Mia Rakic supervision, writing—review and editing. All authors have read and agreed to the published version of the manuscript.

CONFLICT OF INTEREST STATEMENT

The authors declare no conflict of interest.

DATA AVAILABILITY STATEMENT

The data that support the findings of this study are available from the corresponding author upon reasonable request.

ORCID

Luigi Canullo https://orcid.org/0000-0001-9875-2929
Mia Rakic https://orcid.org/0000-0001-7093-7956

REFERENCES

1. Thoma DS, Naenni N, Figuero E, et al. Effects of soft tissue augmentation procedures on peri-implant health or disease: a systematic review and meta-analysis. *Clin Oral Implants Res*. 2018;29:32-49.
2. Avila-Ortiz G, Gonzalez-Martin O, Couso-Queiruga E, Wang HL. The peri-implant phenotype. *J Periodontol*. 2020;91(3):283-288.

3. Monje A, Blasi G. Significance of keratinized mucosa/gingiva on peri-implant and adjacent periodontal conditions in erratic maintenance compliers. *J Periodontol*. 2019;90(5):445-453.
4. Tavelli L, Barootchi S, Avila-Ortiz G, Urban IA, Giannobile WV, Wang HL. Peri-implant soft tissue phenotype modification and its impact on peri-implant health: a systematic review and network meta-analysis. *J Periodontol*. 2021;92(1):21-44.
5. Jain SS, Schramm ST, Siddiqui DA, et al. Effects of multiple implantations of titanium healing abutments: surface characteristics and microbial colonization. *Dent Mater*. 2020;36(9):e279-e291.
6. Zhao B, van der Mei HC, Subbiahdoss G, et al. Soft tissue integration versus early biofilm formation on different dental implant materials. *Dent Mater*. 2014;30(7):716-727.
7. Wang X, Wang Y, Bosshardt DD, Miron RJ, Zhang Y. The role of macrophage polarization on fibroblast behavior – an in vitro investigation on titanium surfaces. *Clin Oral Investig*. 2018;22:847-857.
8. Galarraga-Vinueza ME, Obreja K, Ramanauskaite A, et al. Macrophage polarization in peri-implantitis lesions. *Clin Oral Investig*. 2021;25(4):2335-2344.
9. Weinreb M, Nemcovsky CE. In vitro models for evaluation of periodontal wound healing/regeneration. *Periodontol 2000*. 2015;68(1):41-54.
10. Yu S, Ding L, Liang D, Luo L. Porphyromonas gingivalis inhibits M2 activation of macrophages by suppressing α-ketoglutarate production in mice. *Mol Oral Microbiol*. 2018;33(5):388-395.
11. Wang Y, Zhang Y, Sculean A, Bosshardt DD, Miron RJ. Macrophage behavior and interplay with gingival fibroblasts cultured on six commercially available titanium, zirconium, and titanium-zirconium dental implants. *Clin Oral Investig*. 2019;23:3219-3227.
12. Wang Y, Qi H, Miron RJ, Zhang Y. Modulating macrophage polarization on titanium implant surface by poly (dopamine)-assisted immobilization of IL4. *Clin Implant Dent Relat Res*. 2019;21(5):977-986.
13. Canullo L, Pesce P, Tronchi M, Fiorellini J, Amari Y, Penarrocha D. Marginal soft tissue stability around conical abutments inserted with the one abutment-one time protocol after 5 years of prosthetic loading. *Clin Implant Dent Relat Res*. 2018;20(6):976-982.
14. Koliaraki V, Prados A, Armaka M, Kollias G. The mesenchymal context in inflammation, immunity and cancer. *Nat Immunol*. 2020;21(9):974-982.
15. Canullo L, Micarelli C, Lembo-Fazio L, Iannello G, Clementini M. Microscopical and microbiologic characterization of customized titanium abutments after different cleaning procedures. *Clin Oral Implants Res*. 2014;25(3):328-336.
16. Dunnill C, Patton T, Brennan J, et al. Reactive oxygen species (ROS) and wound healing: the functional role of ROS and emerging ROS-modulating technologies for augmentation of the healing process. *Int Wound J*. 2017;14(1):89-96.
17. Pesce P, Menini M, Santori G, Giovanni ED, Bagnasco F, Canullo L. Photo and plasma activation of dental implant titanium surfaces. A systematic review with meta-analysis of pre-clinical studies. *J Clin Med*. 2020;9(9):2817.
18. Ulbin-Figlewicz N, Jarmoluk A, Marycz K. Antimicrobial activity of low-pressure plasma treatment against selected foodborne bacteria and meat microbiota. *Ann Microbiol*. 2015;65(3):1537-1546.
19. Duske K, Koban I, Kindel E, et al. Atmospheric plasma enhances wettability and cell spreading on dental implant metals. *J Clin Periodontol*. 2012;39(4):400-407.
20. Pistilli R, Genova T, Canullo L, et al. Effect of bioactivation on traditional surfaces and zirconium nitride: adhesion and proliferation of preosteoblastic cells and bacteria. *Int J Oral Maxillofac Implants*. 2018;33:1247-1254.
21. Zhao G, Schwartz Z, Wieland M, et al. High surface energy enhances cell response to titanium substrate microstructure. *J Biomed Mater Res A*. 2005;74(1):49-58.
22. Canullo L, Menini M, Santori G, Rakic M, Sculean A, Pesce P. Titanium abutment surface modifications and peri-implant tissue behavior: a systematic review and meta-analysis. *Clin Oral Investig*. 2020;24(3):1113-1124.
23. Jablonowski L, Fricke K, Matthes R, et al. Removal of naturally grown human biofilm with an atmospheric pressure plasma jet: an in-vitro study. *J Biophotonics*. 2017;10(5):718-726.
24. Matthes R, Duske K, Kebede TG, et al. Osteoblast growth, after cleaning of biofilm-covered titanium discs with air-polishing and cold plasma. *J Clin Periodontol*. 2017;44(6):672-680.
25. Canullo L, Cassinelli C, Götz W, Tarnow D. Plasma of argon accelerates murine fibroblast adhesion in early stages of titanium disk colonization. *Int J Oral Maxillofac Implants*. 2013;28(4):957-962.
26. Griffin M, Palgrave R, Baldovino-Medrano VG, Butler PE, Kalaskar DM. Argon plasma improves the tissue integration and angiogenesis of subcutaneous implants by modifying surface chemistry and topography. *Int J Nanomedicine*. 2018;13:6123-6141.
27. Zhu X, Chian KS, Chan-Park MBE, Lee ST. Effect of argon-plasma treatment on proliferation of human-skin-derived fibroblast on chitosan membrane in vitro. *J Biomed Mater Res A*. 2005;73(3):264-274.
28. Canullo L, Rakic M, Corvino E, et al. Effect of argon plasma pretreatment of healing abutments on peri-implant microbiome and soft tissue integration: a proof-of-concept randomized study. *BMC Oral Health*. 2023;23(1):1-14.
29. General Assembly of the World Medical Association. World medical association declaration of Helsinki: ethical principles for medical research involving human subjects. *J Am Coll Dent*. 2014;81(3):14-18.
30. Silness J, Löe H. Periodontal disease in pregnancy II. Correlation between oral hygiene and periodontal condition. *Acta Odontol Scand*. 1964;22(1):121-135.
31. Ainamo J, Bay I. Problems and proposals for recording gingivitis and plaque. *Int Dent J*. 1975;25(4):229-235.
32. Canullo L, Penarrocha Oltra D, Pesce P, et al. Soft tissue integration of different abutment surfaces: an experimental study with histological analysis. *Clin Oral Implants Res*. 2021;32(8):928-940. doi:10.1111/clr.13782
33. Eckes B, Colucci-Guyon E, Smola H, et al. Impaired wound healing in embryonic and adult mice lacking vimentin. *J Cell Sci*. 2000;113(13):2455-2462.
34. Lim J, Thiery JP. Epithelial-mesenchymal transitions: insights from development. *Development*. 2012;139(19):3471-3486.
35. Hanahan D, Weinberg RA. The hallmarks of cancer. *Cell*. 2000;100(1):57-70.
36. Volk SW, Iqbal SA, Bayat A. Interactions of the extracellular matrix and progenitor cells in cutaneous wound healing. *Adv Wound Care*. 2013;2(6):261-272.
37. Varghese F, Bukhari AB, Malhotra R, De A. IHC profiler: an open source plugin for the quantitative evaluation and automated scoring of immunohistochemistry images of human tissue samples. *PloS One*. 2014;9(5):e96801.
38. Schindelin J, Arganda-Carreras I, Frise E, et al. Fiji: an open-source platform for biological-image analysis. *Nat Methods*. 2012;9(7):676-682.
39. Spieler B, Giret TM, Welford S, Totiger TM, Mihaylov IB. Lung inflammation predictors in combined immune checkpoint-inhibitor and radiation therapy—proof-of-concept animal study. *Biomedicine*. 2022;10(5):1173.
40. Akinshipo AO, Effiom OA, Odukoya O, Akintoye SO. Consistency of color-deconvolution for analysis of image intensity of alpha smooth muscle actin-positive myofibroblasts in solid multicystic ameloblastomas. *Biotech Histochem*. 2020;95(6):411-417.
41. Ruifrok AC, Johnston DA. Quantification of histochemical staining by color deconvolution. *Anal Quant Cytol Histol*. 2001;23(4):291-299.

42. Han J, Pei J, Kamber M. *Data Mining: Concepts and Techniques*. Elsevier; 2011.
43. Quinlan JR. *C4.5: Program for Machine Learning*. Elsevier Science; 1993.
44. Al Rezk F, Trimpou G, Lauer HC, Weigl P, Krockow N. Response of soft tissue to different abutment materials with different surface topographies: a review of the literature. *Gen Dent*. 2018; 66(1):18-25.
45. van Brakel R, Meijer GJ, Verhoeven JW, Jansen J, de Putter C, Cune MS. Soft tissue response to zirconia and titanium implant abutments: an in vivo within-subject comparison. *J Clin Periodontol*. 2012; 39(10):995-1001.
46. Arciola CR, Campoccia D, Montanaro L. Implant infections: adhesion, biofilm formation and immune evasion. *Nat Rev Microbiol*. 2018;16(7): 397-409.
47. Wasy A, Balakrishnan G, Lee SH, et al. Argon plasma treatment on metal substrates and effects on diamond-like carbon (DLC) coating properties. *Cryst Res Technol*. 2014;49(1):55-62.
48. Grundmeier G, Stratmann M. Influence of oxygen and argon plasma treatments on the chemical structure and redox state of oxide covered iron. *Appl Surf Sci*. 1999;141(1–2):43-56.
49. Garlet GP, Giannobile WV. Macrophages: the bridge between inflammation resolution and tissue repair? *J Dent Res*. 2018;97(10):1079-1081.
50. Komori T, Ono M, Hara ES, et al. Type IV collagen α6 chain is a regulator of keratin 10 in keratinization of oral mucosal epithelium. *Sci Rep*. 2018;8(1):1-11.
51. Hollander DA, Erli HJ, Theisen A, Falk S, Kreck T, Müller S. Standardized qualitative evaluation of scar tissue properties in an animal wound healing model. *Wound Repair Regen*. 2003;11(2):150-157.
52. Rodrigues M, Kosaric N, Bonham CA, Gurtner GC. Wound healing: a cellular perspective. *Physiol Rev*. 2019;99(1):665-706.
53. Garcia B, Camacho F, Peñarrocha D, Tallarico M, Perez S, Canullo L. Influence of plasma cleaning procedure on the interaction between soft tissue and abutments: a randomized controlled histologic study. *Clin Oral Implants Res*. 2017;28(10):1269-1277.
54. Siddiqi A, Payne AG, De Silva RK, Duncan WJ. Titanium allergy: could it affect dental implant integration? *Clin Oral Implants Res*. 2011;22(7): 673-680.
55. Wang Y, Zhang Y, Miron RJ. Health, maintenance, and recovery of soft tissues around implants. *Clin Implant Dent Relat Res*. 2016;18(3): 618-634.
56. Cairo F, Nieri M, Cavalcanti R, et al. Marginal soft tissue recession after lateral guided bone regeneration at implant site: a long-term study with at least 5 years of loading. *Clin Oral Implants Res*. 2020; 31(11):1116-1124.
57. Huang HM, Hsieh SC, Teng NC, Feng SW, Ou KL, Chang WJ. Biological surface modification of titanium surfaces using glow discharge plasma. *Med Biol Eng Comput*. 2011;49(6):701-706.
58. Canullo L, Annunziata M, Pesce P, Tommasato G, Nastri L, Guida L. Influence of abutment material and modifications on peri-implant soft-tissue attachment: a systematic review and meta-analysis of histological animal studies. *J Prosthet Dent*. 2021;125(3):426-436.
59. Corvino E, Pesce P, Mura R, Marcano E, Canullo L. Influence of modified titanium abutment surface on peri-implant soft tissue behavior: a systematic review of in vitro studies. *Int J Oral Maxillofac Implants*. 2020;35(3):503-519.
60. Canullo L, Genova T, Tallarico M, Gautier G, Mussano F, Botticelli D. Plasma of argon affects the earliest biological response of different implant surfaces: an in vitro comparative study. *J Dent Res*. 2016; 95(5):566-573.
61. Canullo L, Genova T, Gross Trujillo E, et al. Fibroblast interaction with different abutment surfaces: in vitro study. *Int J Mol Sci*. 2020;21(6): 1919.
62. Ley C, Martin RK, Pareek A, Groll A, Seil R, Tischer T. Machine learning and conventional statistics: making sense of the differences. *Knee Surg Sports Traumatol Arthrosc*. 2022;30(3):753-757.
63. Canullo L, Menini M, Santori G, Rakic M, Sculean A, Pesce P. Titanium abutment surface modifications and peri-implant tissue behaviour. A systematic review and meta-analysis. *Clin Oral Investig*. 2020;24:1113-1124.
64. Sanz-Martín I, Sanz-Sánchez I, Carrillo de Albornoz A, Figuero E, Sanz M. Effects of modified abutment characteristics on peri-implant soft tissue health: a systematic review and meta-analysis. *Clin Oral Implants Res*. 2018;29(1):118-129.

How to cite this article: Canullo L, Donato A, Savadori P, Radovanovic S, Iacono R, Rakic M. Effect of argon plasma abutment activation on soft tissue healing: RCT with histological assessment. *Clin Implant Dent Relat Res*. 2023; 1-11. doi:10.1111/cid.13286